

## Titanium Catalysis | Hot Paper |

## How a Thermally Unstable Metal Hydrido Complex Can Yield High Catalytic Activity Even at Elevated Temperatures

Christian Ehm,<sup>[b]</sup> Juliane Krüger,<sup>[a]</sup> and Dieter Lentz<sup>\*[a]</sup>

**Abstract:** Despite their instability in ethereal solvents, organotitanium hydride catalysts are successfully employed in catalysis at moderate to high temperatures (110 °C), even in the presence of alcohols. It is shown computationally (bond dissociation energy (BDE) analysis and energetic profile for regeneration) and experimentally (EPR studies and kinetic studies), with the specific example of hydrodefluorination (HDF), that despite the long standing belief, regeneration of

Ti–H bonds from Ti–F bonds using silanes is endergonic. The resulting low concentration of Ti–H species is crucial for the catalytic stability of those systems. The resting state in the catalysis is a Ti–F species. The most promising silanes for regeneration are not the ones that have the strongest Si–F bond, but the ones that show the largest difference in Si–F and Si–H BDEs.

## Introduction

Organotitanium hydrides represent a highly reactive class of compounds thought to be the active species in various catalytic processes such as silane dehydrocoupling, olefin hydrogenation, hydrosilylation, and hydrodefluorination (HDF).<sup>[1]</sup>

The reactivity of such Lewis acidic compounds strongly depends on their molecular structure. Titanocene hydride (**1**) forms  $\mu$ -H bridged dimers in the solid state as well as in solution (at ca. –70 °C).<sup>[2]</sup> By warming a THF solution of (Cp<sub>2</sub>TiH)<sub>2</sub> to –30 °C, formation of monomeric Cp<sub>2</sub>TiH(THF) is observed, which decays rapidly via ethereal cleavage yielding the corresponding alkoxy species. Decomposition of (Cp<sub>2</sub>TiH)<sub>2</sub> occurs even in aliphatic solvents like hexane.<sup>[2]</sup> The fluorinated derivative Cp<sub>2</sub>TiF, in contrast, is stable in solution at room temperature, and forms a trimer with a coplanar cyclic (Ti–F)<sub>3</sub> unit.<sup>[3]</sup> It crystallizes in the presence of THF without adduct formation. Several other terminal titanium(III) hydrides bearing sterically demanding Cp\* or Cp' (Cp' = (1,3-Me<sub>3</sub>C)<sub>2</sub>C<sub>5</sub>H<sub>3</sub> or C<sub>5</sub>Me<sub>4</sub>Ph) ligands and/or possessing a Lewis base in the coordination sphere of the metal are known, are thermally stable, and commonly exist in monomeric form.<sup>[4]</sup> Only **1** and other bis-cyclopentadienyl derivatives have been successfully employed in catalysis, however.

In the case of hydrosilylation and HDF, synthetic procedures have been published utilizing Ti<sup>IV</sup>-difluorides as catalyst precursors for catalytically active Ti<sup>III</sup>-hydrides; activation is achieved using a variety of silanes.<sup>[5]</sup> Cp<sub>2</sub>TiH (**1**) or Cp<sub>2</sub>TiH(THF) (**1-THF**) has been described as the active species for hydrosilylation or HDF at temperatures up to 110 °C.<sup>[5]</sup> Contrary to this, Bercaw and Brintzinger observed ether cleavage in **1-THF** even at –30 °C.<sup>[2]</sup>

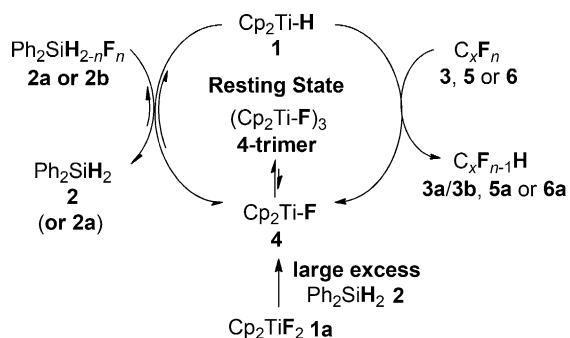
In the specific case of HDF, stoichiometric activation of strong C–F bonds with metal hydrides can be achieved with early as well as late transition metals (TM).<sup>[6]</sup> Catalytic C–F bond activation is, however, often hampered by strong transition metal–fluorine bonds affecting the regeneration of the catalyst. Silanes proved to be very effective in this regard for both early and late TM; this is somewhat surprising because the silane could also be dehydrocoupled or polymerized by the catalyst.<sup>[1]</sup> In 2010, we reported the first Ti-catalyzed HDF of fluoroalkenes (Scheme 1, updated catalytic cycle).<sup>[5]</sup> Subsequently, we gained valuable insight into the regioselectivity of alkene HDF<sup>[3]</sup>, as well as the regioselectivity and mechanism of arene HDF for **1**.<sup>[7]</sup> Several experimental observations indicated that the active species is indeed **1-THF**.<sup>[8]</sup> The discrepancy between the alleged stability of **1-THF** under catalytic conditions and its instability when prepared separately, point to catalyst regeneration playing a vital role.

Bond dissociation energies are the foundation of what is commonly known as 'chemical intuition'. Accurate knowledge of BDEs allows the prediction of reaction energetics, and thus reactivity. Strong bonds are often viewed as inert or 'hard to activate,' and the formation of strong bonds is seen as a potential driving force for reactions. Subsequently, it is commonly accepted that the driving force for catalyst regeneration in HDF reactions can be the Si–F bond strength, as Si–F bonds are stronger than most metal fluoride bonds.<sup>[9]</sup> Employing silanes as hydride sources can convert Ti–F species to hydrides, thus

[a] J. Krüger, Prof. Dr. D. Lentz  
Institut für Chemie und Biochemie, Anorganische Chemie  
Freie Universität Berlin  
Fabeckstr. 34–36, 14195 Berlin (Germany)  
E-mail: dieter.lentz@fu-berlin.de

[b] Dr. C. Ehm  
Dipartimento di Scienze Chimiche  
Università di Napoli Federico II  
Via Cintia, 80126 Napoli (Italy)

Supporting information and the ORCID identification number for the corresponding author of this article are available on the WWW under <http://dx.doi.org/10.1002/chem.201601641>.



**Scheme 1.** Catalytic cycle for HDF of fluorinated substrates, including the importance of endergonic regeneration.  $\text{Ph}_2\text{SiHF}$  (**2a**),  $\text{Ph}_2\text{SiF}_2$  (**2b**), hexafluoropropene (**3**), 1,2,3,4,5-pentafluorotoluene (**5**), perfluorotoluene (**6**), and their corresponding HDF products *E*(**3a**)- and *Z*(**3b**)- pentafluoropropene, 1,2,4,5-tetrafluoro-3-methyltoluene (**5a**) and 1,2,4,5-tetrafluoro-3-(trifluoromethyl)-benzene (**6a**). In donor solvents **1** exists as **1-donor** and **4** as **4-donor**.

yielding catalytic activity. In the following, we will show that based on BDE arguments, regeneration of Ti–H bonds via silanes is endergonic, and we will present computational and experimental evidence for the importance of a Ti–F resting state in HDF catalysis using **1**.

## Results and Discussion

### BDE analysis

The driving force of a reaction of the type depicted in Equation (1a) is, however, the difference in relative BDEs of the pairs EX/EY and E'X/E'Y (E, E', X, Y = different groups or atoms), that is, the difference between the energies of the bonds that are broken and newly formed.



For the specific example considered here, the difference ( $\Delta E_{\text{BDE}}$ ) in relative Ti–H/Ti–F ( $|\Delta E_{\text{Ti}}|$ ) versus Si–H/Si–F ( $|\Delta E_{\text{Si}}|$ ) bond strengths has to be considered [Eq. (1b)].

$$\begin{aligned} \Delta E_{\text{BDE}} &= \text{BDE}_{\text{Ti-F}} + \text{BDE}_{\text{Si-H}} - \text{BDE}_{\text{Ti-H}} - \text{BDE}_{\text{Si-F}} \\ &= (\text{BDE}_{\text{Ti-F}} - \text{BDE}_{\text{Ti-H}}) + (\text{BDE}_{\text{Si-H}} - \text{BDE}_{\text{Si-F}}) \\ &= |\Delta E_{\text{Ti}}| - |\Delta E_{\text{Si}}| \end{aligned} \quad (1b)$$

Experimental titanium hydride bond strengths are unavailable. Therefore, we calculated the BDE data for several silanes and Ti complexes using DFT (gasphase; Table 1).<sup>[10]</sup> Available experimental BDE data for Si–H, Si–F, and Ti–F bonds are in good agreement with DFT predictions. Note that the only available experimental BDE for  $\text{TiF}_3$  is flawed owing to the use of an outdated value in the original BDE calculation.<sup>[9,11,12]</sup> We re-estimated the BDE (see Table 1).

Interestingly, for silane/titanium(III) H–F exchange, BDE considerations predict a highly endergonic reaction. The Ti–F bond is much stronger than the Ti–H bond (by  $\sim 78 \text{ kcal mol}^{-1}$ ), while for Si–F/Si–H the difference amounts to 'only'  $\sim 62 \text{ kcal}$

Table 1. Calculated and experimentally available Si–H, Si–F, Ti–H and Ti–F bond dissociation energies for silanes and titanium species in $\text{kcal mol}^{-1}$ .						
Si–H	$\text{R}_2\text{HSi–H}$		$\text{R}_2\text{FSi–H}$		$\text{R}_3\text{Si–H}$	
R =	Me	Ph	Me	Ph	Me	EtO
calc.	91.1	88.3	93.5	91.6	91.9	95.6
exp.	$93.5 \pm 1.2$	$90.6 \pm 1.6$			$94.7 \pm 1.0$	
Si–F	$\text{R}_2\text{FSi–F}$		$\text{R}_2\text{HSi–F}$		$\text{R}_3\text{Si–F}$	
calc.	160.4	157.7	153.8	150.4	156.6	162.5
exp.					$159.9 \pm 4.8$	
Ti <sup>III</sup>	$\text{Cp}_2\text{Ti–H}$		$\text{Cp}_2\text{Ti–F}$		$\text{F}_2\text{Ti–F}$	
calc.	71.7		150.3		138.0	
exp.					$\sim 138^{[a]}$	
Ti <sup>IV</sup>	$\text{Cp}_2\text{HTi–H}$		$\text{Cp}_2\text{FTi–H}$		$\text{Cp}_2\text{HTi–F}$	
calc.	50.3	39.4	117.8	94.6	116.8	
exp.					$109 \pm 5$	

[a] Ref. [9] gives a value of  $155 \pm 5 \text{ kcal mol}^{-1}$  based on Ref. [11]. The latter reference uses an outdated value for  $\Delta H_f(\text{TiF}_3) = 338.1 \text{ kcal mol}^{-1}$  to calculate the BDE, while the latest NIST recommendation is  $283 \text{ kcal mol}^{-1}$ .<sup>[12]</sup> This led to a severe overestimation of the Ti<sup>III</sup>–F bond energy in Ref. [9] and [11].

$\text{mol}^{-1}$  for the first H–F exchange (secondary silanes), resulting in  $\Delta E_{\text{BDE}}(\text{Regeneration})$  of  $+16 \text{ kcal mol}^{-1}$  [Eq. (1c)].

$$\begin{aligned} \Delta E_{\text{BDE}} &= |\Delta E_{\text{Ti}}| - |\Delta E_{\text{Si}}| \\ &= 78.4 \text{ kcal mol}^{-1} - 62.0 \text{ kcal mol}^{-1} \\ &= 16.4 \text{ kcal mol}^{-1} \end{aligned} \quad (1c)$$

Subsequently, the regeneration step of the catalytic cycle is endergonic, not exergonic as previously assumed.<sup>[13]</sup> In contrast, regeneration for late TM HDF cycles is exergonic, as reported by Macgregor and Whittlesey.<sup>[14]</sup> The overall catalytic cycle is driven by the transformation of C–F into C–H and Si–F into Si–H bonds since  $|\Delta E_{\text{C}}| \ll |\Delta E_{\text{Si}}|$ . The best substrates for regeneration are the ones that show the largest difference in E–F and E–H BDEs, not necessarily the ones that have the strongest E–F bonds. Alanes, for example, have weaker E–H bonds but almost equally strong E–F bonds compared to silanes, and have been successfully used in catalytic HDF reactions.<sup>[9,15]</sup> Finally, it appears that electron-withdrawing substituents on silicon increase the energy difference between Si–F and Si–H bonds (Table 2). This is supported by reports of Buchwald that addition of MeOH to hydrosilylation reactions of **1** enhance the rate due to formation of  $(\text{MeO})_x\text{Si–H}$  species.<sup>[5b]</sup>

Table 2. BDE differences for Si–F/Si–H substitution $ \Delta E_{\text{BDE}} $ in $\text{kcal mol}^{-1}$ .						
$\text{R}_3\text{Si–}$ or $\text{R}_2\text{XSi–}$	$\text{Me}_2\text{HSi}$	$\text{Ph}_2\text{HSi}$	$\text{Me}_2\text{FSi}$	$\text{Ph}_2\text{FSi}$	$\text{Me}_3\text{Si}$	$\text{EtO}_3\text{Si}$
$ \Delta E_{\text{BDE}} $	62.7	62.1	66.9	66.1	64.7	66.9

Fully in line with the straightforward activation of **1a** using silanes, Ti<sup>IV</sup>-mono and -dihydrides are predicted to have even weaker Ti–H bonds than **1**.<sup>[16]</sup> The Ti–F bond in TiF<sub>3</sub> is much stronger than in TiF<sub>4</sub> (Table 1). Similarly, for experimentally available Ti–C BDEs in Cp<sub>2</sub>TiR<sub>2</sub> (R = Me, Ph) systems, the second Ti–C dissociation energy (the Ti<sup>III</sup> bond strength) is also always higher; the same goes for Ti–Cl bonds in TiCl<sub>4</sub>.<sup>[17]</sup>

### Energetic profile of Ti-H regeneration

DFT predicts regeneration of the catalyst (**4** to **1**) to be substantially endergonic [Eqs. (2) and (3)] in solution (PCM model, 298 K) for both Me<sub>2</sub>SiH<sub>2</sub> (computational model) as well as **2**.



The reverse barrier (F–H exchange) is substantially smaller (10 kcal mol<sup>-1</sup>) and regeneration is reversible. The energetic profile for regeneration with Me<sub>2</sub>SiH<sub>2</sub> is shown in Figure 1. The trimer of **4** (**4-trimer**) is predicted to be the resting state (coplanar cyclo-(Ti–F)<sub>3</sub>). The crystal structure as well as the space filling model of **4-trimer** is shown in Figure 2.

H–F exchange via aSBM TS at **4-monomer** with pentacoordinated Si has a barrier of 21.7 kcal mol<sup>-1</sup> (at standard conditions). However, an additional barrier of 4.6 kcal mol<sup>-1</sup> has to be taken into account for the dissociation of **4-trimer**. Regeneration at **4-trimer** through SBM is not possible, as the (Ti–F)<sub>3</sub> unit is effectively shielded by the Cp rings, and a vacant coordination side at Ti is only generated via dissociation.<sup>[19]</sup> This

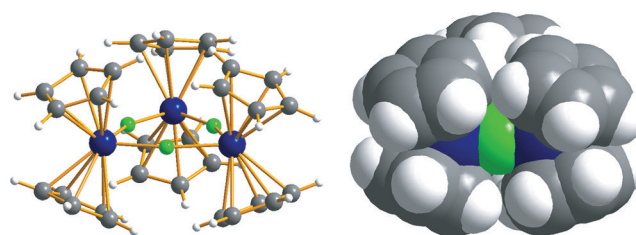


Figure 2. Molecular structure (left) and space filling model (right)<sup>[18]</sup> of **4-trimer** emphasising the shielded Ti environment. Based on data in Ref. [3].

partially compensates the entropic penalty of forming the regeneration TS. The amount of **1-THF** at any given point is exceedingly low. Catalytic turnover is achieved only by HDF.<sup>[20]</sup>

Catalyst decomposition of **1-THF** through THF ring opening is predicted to have a sizable but accessible barrier of 33.2 kcal mol<sup>-1</sup> with no entropic penalty, as THF is the solvent. The barrier is significantly higher from **4-trimer** (52.2 kcal mol<sup>-1</sup>), explaining the stability of the catalytic system over prolonged times at high temperatures. HDF barriers for fluorinated substrates are strongly substrate dependent, but decomposition via THF ring opening can become competitive for less reactive substrates.

Recently, Raza and Braun reported reversible Si–F bond formation at FSi(OEt)<sub>3</sub> promoted by Rh<sup>I</sup> complexes.<sup>[21]</sup> In light of our results, this indicates that reversibility in Si–F bond formation might be more common than previously assumed, albeit one of the strongest element–fluorine bonds known. The kinetic profile is sensitive to concentration changes, and a more realistic profile for initial catalytic concentrations of catalyst and substrates is also shown in Figure 1.

The energetic profile has some major kinetic consequences:

- 1) Highly concentrated solutions are needed to achieve acceptable TOF, because regeneration TS (**TS4-1**) as well as HDF TS are formed without prior adduct formation.<sup>[3,5,7]</sup>
- 2) Substrates with a low HDF barrier constantly remove **1-THF** from the equilibrium, shifting it in the direction of **1-THF**.
- 3) As the silane is consumed, the forward regeneration barrier rises, since the entropy contribution to the TS increases. Thus, an excess of silane is needed to drive HDF reactions to full conversion.<sup>[3,5,7]</sup>
- 4) Whether regeneration or HDF is the rate-limiting step depends on the specific barrier for HDF.
- 5) When HDF is the rate limiting step, the overall barrier is composed of the exchange part (regeneration) and the C–F activation barrier.
- 6) The equilibrium of **1-THF** and **4-trimer** heavily affects overall barrier heights and is solvent dependent.

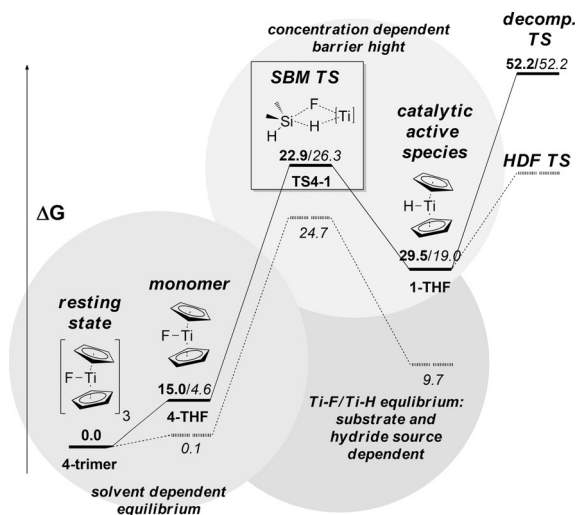


Figure 1. Enthalpy (bold values) and Gibbs Free Energy (italic values) profile for regeneration of the catalyst in kcal mol<sup>-1</sup> (298 K, THF). Bold profile: standard conditions, dashed profile for realistic concentrations: Me<sub>2</sub>SiH<sub>2</sub> (5 × 10<sup>-1</sup> mol L<sup>-1</sup>) ≫ [Cp<sub>2</sub>TiF<sub>3</sub>] (5 × 10<sup>-3</sup> mol L<sup>-1</sup>) ≫ Cp<sub>2</sub>TiF (5 × 10<sup>-4</sup> mol L<sup>-1</sup>) ≫ Cp<sub>2</sub>TiH (5 × 10<sup>-5</sup> mol L<sup>-1</sup>) and Me<sub>2</sub>SiH<sub>2</sub> > Me<sub>2</sub>SiHF (5 × 10<sup>-3</sup> mol L<sup>-1</sup>). Level of theory M06-2X(PCM)/TZ//M06-2X(PCM)/DZ (SBM TS = σ-bond metathesis transition state, HDF TS = hydrodefluorination transition state). Lowest HDF TS and decomposition TS are only shown as orientation.

### Experimental studies

As predicted by DFT, experimental kinetics are affected by the choice of solvent (Table 3). More basic ethers (e.g., THF) lead to higher TOF than less basic ethers (e.g., diglyme) or even aro-

substrate	solvent (2 mL)	conv. [%]	1 a [mol%]	2 [equiv]	T [°C]	t [h]	TOF [h <sup>-1</sup> ]
3	toluene	traces	0.7	1.1	rt	0.25	< 1
3	toluene	72	2	1.5	110	24	1.4
3	diglyme	79	0.6	1.1	rt	0.25	530
5	diglyme	20	15	5	110	72	1.9 × 10 <sup>-2</sup>
5	dioxane	30	15	5	110	96	2.1 × 10 <sup>-2</sup>
5	THF	100	15	5	110	96	7 × 10 <sup>-2</sup>

matic solvents. Donor solvents are not critically needed but reduce the overall barrier. The choice of solvent can be crucial in case of unreactive substrates like **5** to achieve full conversion within reasonable reaction times.

We also tested triethoxysilane (**2c**) as a hydride source in the HDF reaction of **3** (Table 4). A color change to dark blue upon addition of **2c** indicates successful reduction of the precatalyst, however, after 15 min at room temperature, no HDF product was observed. Activation of the precatalyst with **2** followed by cooling to -35 °C and subsequent addition of **3** and **2c**, yields a TOF of 12 h<sup>-1</sup>, surpassing the TOF of 0.7 h<sup>-1</sup> at -25 °C achieved in kinetic experiments with **2** alone. We tentatively conclude that alkoxy silanes lower the regeneration barrier as predicted by BDE arguments, but accelerate catalyst decomposition to alkoxytitanium compounds.

substrate	solvent (2 mL)	conv. [%]	1 a [mol%]	2 c [equiv]	T [°C]	t [h]	TOF [h <sup>-1</sup> ]
3	diglyme	0	3.0	1.3	rt	0.25	0
3	diglyme	2	1.1	1.0 <sup>[a]</sup>	-70	1	2
3	diglyme	13	1.1	1.0 <sup>[a]</sup>	-35	1	12

[a] Plus 1.2 equiv of **2**.

EPR spectra of the catalytic reaction mixture are shown in Figure 3, and were taken before (A) and after addition of the perfluorinated substrate (B). HDF of perfluorotoluene (**6**) is slow enough to allow a catalytic EPR study at room temperature. Prior to the reaction, a featureless broad singlet is observed. This is consistent with a Ti-alkoxide (Cp<sub>2</sub>Ti-ONBu) as the major decomposition product of **1-THF**.<sup>[2]</sup> The *g*-value of 1.987 is in line with literature data for Cp<sub>2</sub>Ti-OMe,<sup>[2b]</sup> and implies the intermediate presence of **1-THF**.<sup>[22]</sup> Furthermore, a smaller signal is buried under the large signal from Cp<sub>2</sub>Ti-ONBu, and this might very well correspond to a doublet from residual amounts of **1-THF** or a silyl species (doublet coupling). Dimeric Ti<sup>III</sup>/Ti<sup>IV</sup> (higher order coupling) species cannot be responsible for the is resonance.

During the reaction (B), a broad singlet with a *g*-value of 1.980, comparable to 1.981 for Cp<sub>2</sub>TiF(PMe<sub>3</sub>), is observed likely corresponding to either **4** or **4-trimer**.<sup>[23]</sup> Similar to other literature examples, the fluorine coupling is too small to be re-

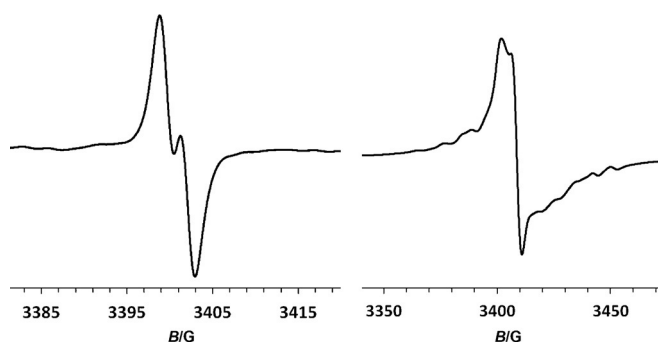


Figure 3. EPR spectra of the activated precatalyst (A) and of the reaction mixture (B) at room temperature. For (A), 0.5 mL of a stock solution with [1 a] = 5 mmol L<sup>-1</sup> and [2] = 0.6 mol L<sup>-1</sup> in 2 mL THF were filled in a glass ampule (4 mm o.d.) degassed and flame sealed. (B) was prepared identically to (A) + 0.16 mmol of **6**.

solved.<sup>[24]</sup> The EPR spectrum (B) remains unchanged over three days (complete conversion of **6**).

Preliminary kinetic studies (-25 °C to -15 °C) under pseudo-zeroth order conditions (large excess of **2** and **3**, max. 10% conversion monitored) yielded activation parameters of ΔH = 20 kcal mol<sup>-1</sup> and ΔS = 7.6 cal mol<sup>-1</sup> K<sup>-1</sup> (Figure 4). The entropy contribution is small.

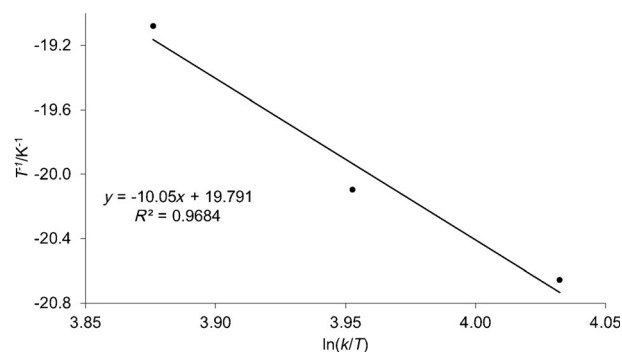
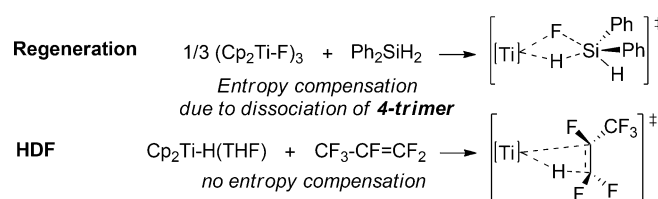


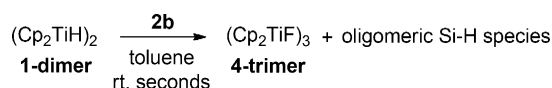
Figure 4. Eyring plot for catalytic HDF of **3** at -15, -20, and -25 °C.

Note that while trimer dissociation can compensate for the entropic penalty of forming a TS out of two independent molecules, release of THF from **1-THF** into the THF solvent should not lead to pronounced entropy compensation (Scheme 2).<sup>[25]</sup> This is fully in line with **4-trimer** and not **1-THF** being the resting state of catalysis.

Independently prepared (Cp<sub>2</sub>TiH)<sub>2</sub> (**1-dimer**) is not stable in the presence of fluorinated silanes (Scheme 3), and yields **4-**



Scheme 2. regeneration TS (top), and HDF TS (bottom).



Scheme 3. Reaction of 1-dimer with 2b.

trimer (identified by EPR) and oligomeric Si species (indicated by the disappearance of fluorosilane **2b** and appearance of several new signals in the polysilane  $^{29}\text{Si}$ -NMR region).

### Effect of endergonic regeneration on catalyst stability

The kinetic profile for regeneration provides an explanation for seemingly contradictory experimental observations by us and Bercaw. Catalytic HDF reactions at RT or higher temperatures are possible in THF (or other ethereal solvents) with the active species being **1-THF** because it is only present in small amounts. The stabilizing effect of endergonic regeneration extends beyond the HDF example presented here. Buchwald's catalyst activation protocol for hydrosilylation, for example, should yield **4** or **4-trimer** in the absence of a substrate, and could explain the high stability of '**1-THF**' even in the presence of methanol.<sup>[3b]</sup> Under catalytic conditions, the amount of fluorosilanes from activation will always be much higher than the amount of free **1-THF**.

### Conclusion

The driving force for catalytic HDF reactions is the BDE difference between C–F/C–H and Si–F/Si–H, respectively, because regeneration is endergonic. DFT predictions are in very good agreement with experimental results. The resting state in HDF catalysis of **1** is the Ti–F species **4-trimer**. The results presented here emphasize that catalyst regeneration in a catalytic cycle does not necessarily have to be exergonic, as long as the overall cycle is exergonic. Endergonic regeneration can actually be beneficial to catalyst stability of very reactive catalysts. The rate-limiting step in such cases consists of a catalyst regeneration and C–F bond activation part.

### Experimental Section

**Calculations:** All structures were fully optimized at the M06–2X(PCM)<sup>[26]</sup>/6–31+(2d,p) level using Gaussian 09<sup>[10]</sup> coupled to an external optimizer (PQS)<sup>[27]</sup> instead of the internal Gaussian optimizer, using an ultrafine grid (Int(Grid=ultrafine)) and standard SCF convergence quality settings (Scf=tight) for Gaussian single-point calculations. The nature of each stationary point was checked with an analytical second-derivative calculation (no imaginary frequency for minima, exactly one imaginary frequency for transition states, corresponding to the reaction coordinate) and the accuracy of the TS was confirmed with IRC scans. S2 values for all doublet species are below 0.77. Solvent influence of polar solvents (THF,  $\epsilon = 4.24$ ) was modeled explicitly, using the polarizable continuum model (PCM) implemented in the Gaussian 09 software suite. Transition states were located using a suitable guess and the Berny algorithm (Opt=TS).<sup>[28]</sup> Vibrational analysis data derived at this level of theory were used to calculate thermal corrections (enthalpy and

entropy, 298 K, 1 bar) for all species considered. Final single-point energies (SP) were calculated at the M06–2X(PCM)<sup>[29]</sup> level of theory employing triple- $\zeta$  Dunning basis sets (cc-pVTZ) from the EMSL basis set exchange library,<sup>[30]</sup> to minimize BSSE contributions.<sup>[31]</sup> BDE calculations were performed similarly but without solvent corrections.

**Techniques:** All reactions and manipulations were carried out in pre-dried glassware under an argon atmosphere by using standard Schlenk-type and vacuum-line techniques, or by working in an argon-filled glovebox. The amount of gaseous compounds was determined using pVT technique or by condensing the gas into a weighted J. Young valve flask.

**Chemicals:** All solvents were distilled from sodium or potassium, and stored over sodium/potassium alloy. **1-Dimer** was prepared in a 50 mL J. Young valve flask similar to the literature procedure.<sup>[2b]</sup> **1a**, **2**, **5**, and **6** were purchased from abcr GmbH, Karlsruhe. **2**, **5**, **6** were distilled over  $\text{CaH}_2$  and **2** was stored in the glove box.  $\text{Ph}_2\text{SiF}_2$  was purified by vacuum distillation at room temperature. **3** (Solvay Fluor) and **2c** (Prof. Braun, HU Berlin) were obtained free of charge, **3** was used as received and **2c** was stored in the glove box.

**Catalytic hydrodefluorination:** Substrates, conditions, conversion and TOF are listed in Tables 3 and 4. A single-necked flask equipped with a J. Young valve was charged with **1a**, **2** (and **2c**) and solvent, and a change in color from yellow to purple to green was observed immediately. The substrate was added with a syringe or condensed into the reaction mixture. Subsequently, the flask was degassed and the corresponding conditions were applied, respectively (cf. Tables 3 and 4). The conversion of the substrates was determined from NMR spectra by integration of product resonances versus the internal standard (fluorobenzene). The products were identified by  $^{19}\text{F}$  NMR spectroscopy ( $[\text{D}_8]$ benzene), using available literature data for **3a**,<sup>[32]</sup> **3b**,<sup>[32]</sup> and **5a**.<sup>[33]</sup>

**Kinetic experiments:** For a stock solution, **1a** (5.5 mg, 25.5  $\mu\text{mol}$ ), **2** (550  $\mu\text{L}$ , 3.0 mmol) and  $[\text{D}_8]$ THF (2 mL) were mixed in the glovebox and stored at  $-40^\circ\text{C}$ . For each sample, 200  $\mu\text{L}$  stock solution was filled in a glass ampule (4 mm outer diameter (o.d.)), degassed, and **3** (115 mg, 0.7 mmol) was added by vacuum transfer; the ampule was flame sealed and subsequently immersed into a cooling bath at  $-78^\circ\text{C}$ . To determine  $G/H/S$ , the reaction progress was monitored by  $^{19}\text{F}$  NMR spectroscopy at  $-15$ ,  $-20$ , and  $-25^\circ\text{C}$ , respectively. The conversion of the substrate was determined from  $^{19}\text{F}$  NMR spectra by integration of product and starting material resonances (detailed data is given in the Supporting Information).

**Reaction of 1-dimer with 2b:** **1-Dimer** (150 mg, 0.422 mmol/0.843 mmol monomeric) was dissolved in  $[\text{D}_8]$ toluene (2 mL) at room temperature. Upon addition of **2b** (88.2  $\mu\text{L}$ , 0.461 mmol) the color changed from violet to green. 0.4 mL of the reaction mixture was used for an NMR experiment. In the  $^{29}\text{Si}$  NMR spectra ( $[\text{D}_8]$ toluene), the initial resonance of  $\text{Ph}_2\text{SiF}_2$  at  $-26.9$  ppm disappeared and four new resonances ( $-33.09$ ,  $-33.45$ ,  $-36.8$ , and  $-37.0$  ppm) in the disilane/polysilane region developed.<sup>[34]</sup> The solvent of the residual mixture was removed under vacuum and an EPR spectra was recorded. EPR (toluene): broad singlet at  $g = 1.976(9)$ , identical to the literature data.<sup>[24]</sup>

### Acknowledgements

The authors would like to thank Prof. P. H. M Budzelaar (U-Manitoba, Winnipeg) for generous donation of CPU time and valuable discussions on the manuscript. Support from the

Deutsche Forschungsgemeinschaft (DFG) is gratefully acknowledged.

**Keywords:** catalyst regeneration · density functional calculations · homogeneous catalysis · hydrodefluorination · metal hydride

- [1] a) A. J. Hoskin, D. W. Stephan, *Coord. Chem. Rev.* **2002**, 233–234, 107; b) J. F. Harrod, *Coord. Chem. Rev.* **2000**, 206–207, 493.
- [2] a) H. Brintzinger, *J. Am. Chem. Soc.* **1967**, 89, 6871–6877; b) J. E. Bercaw, H. Brintzinger, *J. Am. Chem. Soc.* **1969**, 91, 7301–7306.
- [3] M. F. Kuehnel, P. Holstein, M. Kliche, J. Krüger, S. Matthies, D. Nitsch, J. Schutt, M. Sparenberg, D. Lentz, *Chem. Eur. J.* **2012**, 18, 10701–10714.
- [4] a) W. W. Lukens, P. T. Matsunaga, R. A. Andersen, *Organometallics* **1998**, 17, 5240–5247; b) G. A. Luinstra, J. H. Teuben, *J. Chem. Soc. Chem. Commun.* **1990**, 1470–1471; c) M. D. Walter, C. D. Sofield, R. A. Andersen, *Organometallics* **2008**, 27, 2959–2970; d) J. M. de Wolf, A. Meetsma, J. H. Teuben, *Organometallics* **1995**, 14, 5466–5468; e) J. W. Pattiasina, F. van Bolhuis, J. H. Teuben, *Angew. Chem. Int. Ed. Engl.* **1987**, 26, 330–331; *Angew. Chem.* **1987**, 99, 342–343; f) S. R. Frerichs, B. K. Stein, J. E. Ellis, *J. Am. Chem. Soc.* **1987**, 109, 5558–5560; g) Y. You, S. R. Wilson, G. S. Girolami, *Organometallics* **1994**, 13, 4655–4657.
- [5] a) M. F. Kuehnel, D. Lentz, *Angew. Chem. Int. Ed.* **2010**, 49, 2933–2936; *Angew. Chem.* **2010**, 122, 2995–2998; b) X. Verdagner, U. E. W. Lange, M. T. Reding, S. L. Buchwald, *J. Am. Chem. Soc.* **1996**, 118, 6784–6785; c) G. Podolan, D. Lentz, H.-U. Reißig, *Angew. Chem. Int. Ed.* **2013**, 52, 9491–9494; *Angew. Chem.* **2013**, 125, 9669–9672.
- [6] a) M. F. Kuehnel, D. Lentz, T. Braun, *Angew. Chem. Int. Ed.* **2013**, 52, 3328–3348; *Angew. Chem.* **2013**, 125, 3412–3433; b) M. Klahn, U. Rosenthal, *Organometallics* **2012**, 31, 1235–1244.
- [7] A manuscript focusing on the studies of HDF barriers for fluorinated arenes and olefins is currently under preparation and will be published in due course.
- [8] The stoichiometric reaction of 1-THF with **3** yielded **3a** and **3b** in the same ratio in the catalytic reaction ( $E/Z=0.67$ ).
- [9] Y.-R. Luo in *Comprehensive handbook of chemical bond energies*, CRC Press, Boca Raton, **2007**.
- [10] a) Further details in the Supporting Information; b) Gaussian 09, Revision B.01, M. J. Frisch, G. W. Trucks, H. B. Schlegel, G. E. Scuseria, M. A. Robb, J. R. Cheeseman, G. Scalmani, V. Barone, B. Mennucci, G. A. Petersson, H. Nakatsuji, M. Caricato, X. Li, H. P. Hratchian, A. F. Izmaylov, J. Bloino, G. Zheng, J. L. Sonnenberg, M. Hada, M. Ehara, K. Toyota, R. Fukuda, J. Hasegawa, M. Ishida, T. Nakajima, Y. Honda, O. Kitao, H. Nakai, T. Vreven, J. A. Montgomery, Jr., J. E. Peralta, F. Ogliaro, M. Bearpark, J. J. Heyd, E. Brothers, K. N. Kudin, V. N. Staroverov, R. Kobayashi, J. Normand, K. Raghavachari, A. Rendell, J. C. Burant, S. S. Iyengar, J. Tomasi, M. Cossi, N. Rega, J. M. Millam, M. Klene, J. E. Knox, J. B. Cross, V. Bakken, C. Adamo, J. Jaramillo, R. Gomperts, R. E. Stratmann, O. Yazyev, A. J. Austin, R. Cammi, C. Pomelli, J. W. Ochterski, R. L. Martin, K. Morokuma, V. G. Zakrzewski, G. A. Voth, P. Salvador, J. J. Dannenberg, S. Dapprich, A. D. Daniels, Ö. Farkas, J. B. Foresman, J. V. Ortiz, J. Cioslowski, D. J. Fox, Gaussian, Inc. Wallingford CT, **2009**.
- [11] K. F. Zmbov, J. L. Margrave, *J. Phys. Chem.* **1967**, 71, 2893–2895.
- [12] M. W. Chase, C. A. Daives, J. R. Downey, D. J. Frurip, R. A. McDonald, A. N. Syverud, in *JANAF Thermochemical Tables, Third Edition* JPCRD 14, Supplement No. 1, **1985**.
- [13] We initially considered that  $Ti^{III}$ -systems might pose some problems for DFT in predicting accurate BDEs. However, for the exchange process, only  $\Delta E_{BDE}$  matters, and though absolute accuracy in BDE might be off, relative accuracy is usually more reliable due to fortuitous error cancellation.
- [14] J. A. Panetier, S. A. Macgregor, M. K. Whittlesey, *Angew. Chem. Int. Ed.* **2011**, 50, 2783–2786; *Angew. Chem.* **2011**, 123, 2835–2838.
- [15] a) U. Jäger-Fiedler, M. Klahn, P. Arndt, W. Baumann, A. Spannberg, V. V. Burkalov, U. Rosenthal, *J. Mol. Catal. A* **2007**, 261, 184–189; b) S. Yow, S. J. Gates, A. J. P. White, M. R. Crimmin, *Angew. Chem. Int. Ed.* **2012**, 51, 12559–12563; *Angew. Chem.* **2012**, 124, 12727–12731.
- [16] a) E. Samuel, J. F. Harrod, *J. Am. Chem. Soc.* **1984**, 106, 1859–1860; b) C. T. Aitken, J. F. Harrod, E. Samuel, *J. Am. Chem. Soc.* **1986**, 108, 4059–4066.
- [17] J. A. M. Simoes, J. L. Beauchamp, *Chem. Rev.* **1990**, 90, 629–688.
- [18] Diamond - Crystal and Molecular Structure Visualization Crystal Impact - Dr. H. Putz & Dr. K. Brandenburg GbR, Kreuzherrenstr. 102, 53227 Bonn, Germany.
- [19] Formation of mixed Ti–F/Ti–H oligomers appears possible but does not affect the energetics of regeneration.
- [20] Details on HDF mechanisms will be published in due course.
- [21] A. L. Raza, T. Braun, *Chem. Sci.* **2015**, 6, 4255–4260.
- [22] It appears plausible that  $Cp_2Ti-OBu$  is the initial resting state if the substrate is not added fast enough. During catalysis, however, the concentration of  $Si-F \gg Si-OBu$ .
- [23] L. Hao, J. F. Harrod, *Inorg. Chem. Commun.* **1999**, 2, 191–194.
- [24] L. Bai, F. Liu, J. Wang, *Sci. China Ser. B* **1991**, 34, 257–264.
- [25] C. Ehm, R. Cipullo, P. H. M. Budzelaar, V. Busico, *Dalton Trans.* **2016**, 45, 6847–6855.
- [26] Y. Zhao, D. G. Truhlar, *Theor. Chem. Acc.* **2008**, 120, 215–241.
- [27] a) J. Baker, *PQS, 2.4 Parallel Quantum Solutions*, Fayetteville, AR, 2001; b) J. Baker, *J. Comput. Chem.* **1986**, 7, 385–395.
- [28] The Berny algorithm was never completely published; see the Gaussian documentation for details, ref.[10].
- [29] a) R. Raucoles, T. de Bruin, P. Raybaud, C. Adamo, *Organometallics* **2009**, 28, 5358–5367; b) S. Tobisch, T. Ziegler, *J. Am. Chem. Soc.* **2004**, 126, 9059–9071.
- [30] a) D. Feller, *J. Comput. Chem.* **1996**, 17, 1571; b) K. L. Schuchardt, B. T. Didier, T. Elsethagen, L. Sun, V. Gurumoorhi, J. Chase, J. Li, T. L. Windus, *J. Chem. Inf. Model.* **2007**, 47, 1045.
- [31] S. F. Boys, F. Bernardi, *Mol. Phys.* **1970**, 19, 553.
- [32] H. Koroniak, K. W. Palmer, W. R. Dolbier, H.-Q. Zhang, *Magn. Reson. Chem.* **1993**, 31, 748–751.
- [33] A. A. Shtark, Yu. V. Pozdnyakovich, V. D. Shteingarts, *Zh. Org. Khim.* **1977**, 13, 1671–1679.
- [34] H. Söllradl, E. Hengge, *J. Organomet. Chem.* **1983**, 243, 257–269.

Received: April 8, 2016

Published online on June 3, 2016